

Simulation of a two-dimensional laser diode array directly cooled by coolant flow

V.A. Oleshchenko, A.P. Bogatov, N.V. D'yachkov, V.V. Bezotosnyi

Abstract. We report an analysis of attained output powers of laser diode bars (LDBs) and power densities of two-dimensional laser diode arrays (LDAs). A new LDA design is proposed and its thermal regime is simulated. The cw output power of the proposed LDA consisting of standard cw LDBs (output power 100 W, efficiency 50%, cavity length 2 mm) can reach 5 kW cm^{-2} . The parameters of a coolant flow in the microchannels of the LDA heat sink necessary to achieve such powers are calculated.

Keywords: laser diode array, coolant, cooling, output power.

1. Introduction

One of the most important directions of the development of modern laser diodes (LDs) is aimed at increasing their output power. Progress in this field is achieved as a result of optimisation of the cavity length and the reflection coefficients of mirrors [1], increase in the efficiency [2], and decrease in the thermal load on the active region. The latter is obtained by improving the methods of mounting of laser chips on heat sinks and by using materials with a rather high thermal conductivity and thermal expansion coefficients matched to those of the laser crystal in order to decrease the thermoelastic stress and increase the cooling efficiency.

The output power of one LD bar (LDB) in the cw regime closely approaches 1 kW at a coolant temperature of 15°C , a total efficiency of 70%, a standard emitting aperture width of 10 mm, and a cavity length of 4 mm [3]. A year earlier, Frevert et al. [4] achieved the optical power from one similar LDB in a pulsed (QCW) regime of 2 kW at a coolant temperature of -70°C and 1 kW at room temperature. The main obstacle to increasing the output powers of LDBs is the extremely high heat flux densities in the cooling system.

Removal of high-density heat fluxes from an LD array (LDA) – two-dimensional array of LDBs – is even a more challenging task. One of the recent achievements of COHERENT-DILAS researchers is the development of an LDA consisting of eight sandwiches (thermal compensator/LDB/thermal compensator), each with a power of 450 W. The LDA output power in the QCW regime was 3.6 kW at a power density of 2.7 kW cm^{-2} [5]. An LDA consisting of

50 LDBs with a power of 250 W each emitted cw radiation with a power density of about 2 kW cm^{-2} at 25°C [5].

A similar result (about 2 kW cm^{-2} in a cw regime) at the total LDA power of 6 kW was obtained in [6]. In this work, special attention was paid to solving the problem of deformations and thermoelastic stresses formed upon operation, and an LDB smile of about $1 \mu\text{m}$ was achieved at an aperture of 10 mm. The smile must be reduced to improve the uniformity of the emitting aperture of LDBs and LDAs for industrial applications.

When analysing the results of works [5, 6], it seems that the power densities of 2 kW cm^{-2} for the cw regime and about 3 kW cm^{-2} for the QCW regime are close to the power density limits for the used structures. The fundamental limits are mainly determined by insufficient thermal conductivity of heat-sink materials and a difference between the thermal expansion coefficients of these materials and semiconductor crystals of LDBs.

In the present work, we consider an LDA design based on a principally new approach to the problems of increasing the LDA cooling efficiency, which consists in direct two-side cooling of LDBs by a coolant in the LDA structure (RF Patent No. 2712764, priority date 11.06.2019, Lebedev Physical Institute, Russian Academy of Sciences, and Inventor's Certificate No. 2020137239, 12.11.2020). In the proposed engineering solution, heat from the LDA was removed directly by a coolant flow due to convection cooling, which is more effective than conductive cooling used in all known LDA structures. We propose an LDA model based on standard home-developed industrial LDBs with a cavity length of 2 mm operating in the cw regime at room temperature [7]. As a basis, we consider an LDA structure with an aperture of $10 \times 10 \text{ mm}$ containing 50 such LDBs.

2. Principal LDA structure and its parameters

A simplified LDA scheme (Fig. 1) shows a fragment consisting of seven LDBs. The dimensions of LDBs (l) are close to standard (thickness $100 \mu\text{m}$, length (aperture) 10 mm, and width (laser cavity length) 2 mm). Each LDB contains 50 emitting clusters, i.e., individual lasers, which fill the LDB aperture with a fill factor of 50%. The LDBs are positioned parallel to each other and spaced by $100 \mu\text{m}$; therefore, the spaces between the LDB crystals and side walls (7) form eight channels in the form of thin-wall tubes with rectangular cross sections for circulation of a coolant directly cooling both metallised sides of the LDBs. The coolant flows indicated in Fig. 1 by arrows 8, can be both unidirectional (UD) and counter-directional (CD) as is shown in Fig. 1 for neighbouring channels. It was shown in [8] on the example of two-layer

V.A. Oleshchenko, A.P. Bogatov, N.V. D'yachkov, V.V. Bezotosnyi
Lebedev Physical Institute, Russian Academy of Sciences, Leninsky
prosp. 53, 119991 Moscow, Russia; e-mail: bezotosnyjvv@lebedev.ru

Received 10 December 2020
Kvantovaya Elektronika 51 (3) 196–200 (2021)
Translated by M.N. Basieva

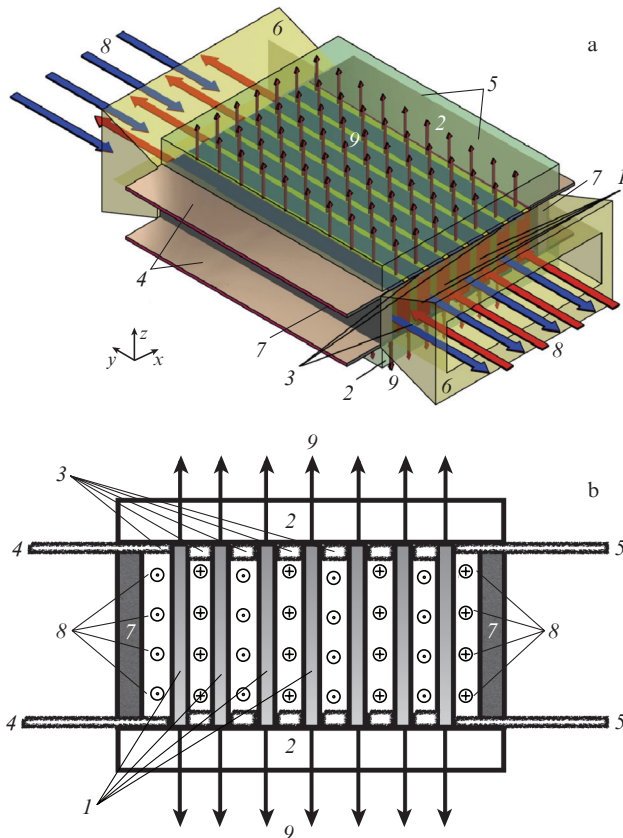


Figure 1. (a) Principal isometric scheme of an LDA with CD coolant flows and (b) its xz cross section: (1) LDB; (2) sapphire plate; (3) conducting metallised coating; (4, 5) contact electrodes; (6) channel funnels; (7) LDA outer walls; (8) CD coolant flows; (9) output radiation.

microchannel heat sinks that the counter propagation of coolant flows additionally increases the heat removal efficiency and improves the thermal field uniformity.

On the side of cavity mirrors, the LDBs are attached to plates 2, which are transparent to the LDB radiation and, in our case, are made of sapphire with a thermal conductivity of $33 \text{ W m}^{-1} \text{ K}^{-1}$. Note that these plates can be made of another transparent material (for example, optical glass) or can be plane faces of solid-state active elements (slabs or disks) pumped by the LDA radiation (arrows 9). Plates 7 are responsible for the mechanical strength of the LDA and encapsulation of the channel system. The LDBs consist mainly of GaAs with a thermal conductivity of $35 \text{ W m}^{-1} \text{ K}^{-1}$. Our calculation takes into account the parameters of all layers of the standard LDBs based on a separate-confinement double heterostructure, as well as the parameters of metallisation layers. This LDA design makes it possible to implement double-side cooling of LDBs and, if necessary, to obtain bidirectional output. The latter can be useful for increasing the LDB power due to increasing its efficiency, because bidirectional output leads to an increase in the ratio between the useful and internal losses.

The LDA was pumped by a current flowing through LDBs connected in series. Electric connection between neighbouring LDBs is provided by the metallisation coating (3) of the walls of channels through which the dielectric coolant flows. The electric circuit is closed by the positive (4) and negative (5) electrodes connected to the power supply.

The heat sources in the model are the active regions of LDBs with the following parameters: thickness 0.1 mm, cw

radiation power 100 W, efficiency 50%, thermal power density removed from each LDB 500 W cm^{-2} , average optical LDA output power density 5 kW cm^{-2} , and initial temperature of the system 20°C . The model takes into account the temperature dependence of the coolant viscosity; as a cooling fluid, we used distilled water, whose temperature parameters are given in [9]. The temperature boundary conditions are as follows: the outer sides of plates 2 (Fig. 1) and the external input and output sides of the coolant supply tube (6) had a stable temperature of 20°C . As is known, for highly efficient heat transfer, it is preferable to use a turbulent coolant flow because it is characterised by a thin near-wall layer and, hence by a larger contribution from the convective cooling mechanism than from the conductive one, which manifests itself in a higher Peclet number defined as the ratio between the rates of these two processes.

To calculate the final stationary distribution of thermal fields and the field of turbulent coolant flow velocities, we used the finite-element method and the Comsol Multiphysics software. To solve the turbulence problem, we used a flow model with automatic selection of near-wall functions, which was used to calculate the dependence of the turbulent viscosity coefficient on the local fluid velocity and the distance to the channel wall with allowance for the fluid temperature. This model is most stable and is characterised by low requirements for computational resources. Division into finite elements was performed automatically; each 58.5-mm^3 volume contained more than 123000 discrete elements in the channels with a liquid coolant. To increase the calculation accuracy, the number of discrete elements near the channel walls was considerably increased.

3. Results of 3D simulation

The coolant flow velocities at the entrance to the inlet rectangular funnel were 10 and 15 m s^{-1} at the residual pressure of 2 atm at the end of the outlet funnel. Figure 2a shows the distribution of the coolant pressure in the xy cross section of the channel, and Fig. 2b presents the average coolant velocity in the xy plane of the channel 0.1 mm in size in the middle of the LDB (see the inset in Fig. 2). These distributions are valid for all channels and both UD and CD flows because the channels are identical and only the coolant flow direction changes. Figure 2a shows that, at the initial coolant flow velocities of 10 and 15 m s^{-1} , the pressure at the entrance to the inlet funnel slightly exceeds 6 and 10 atm, respectively, but the pressure in the channels between LDBs considerably decreases and is equal to 5 and 7 atm at the entrance and less than 1.5 and 0.3 atm at the exit. The higher the pressure at the entrance to the inlet funnel, the lower the pressure at the exit from the channel, which testifies to the turbulent character of the flow at the increased pressure. The simulation showed that an increase in the pressure at the entrance to the channel above 10 atm leads to the possibility of formation of a low-pressure region at the exit region and to the appearance of cavitation and air bubbles.

From the viewpoint of the LDA operation reliability, the cavitation regime is unacceptable and, in addition, the pressure exceeding 10 atm raises requirements to the mechanical strength of the structural elements, which may cause technical problems; therefore, in simulation, we did not use input pressures exceeding 10 atm. Analysis of Comsol simulations [10] showed that, in the chosen ranges of pressures and flow velocities, the influence of the mentioned low-pressure regions on

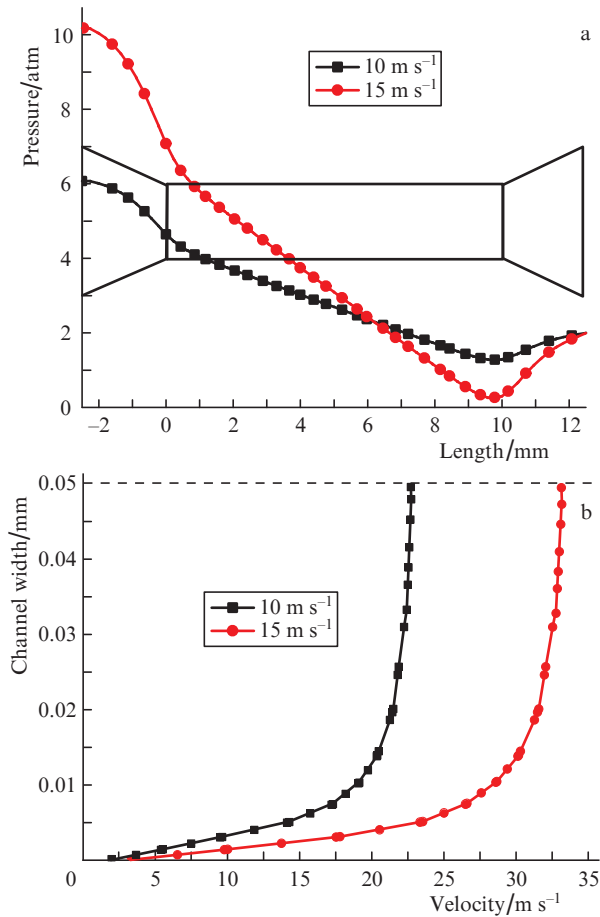


Figure 2. (a) Distribution of the coolant pressure in the cooling system and cross-section of the funnel–channel–funnel system coordinated with the plot, as well as (b) coolant velocity distribution in the central region of the channel in the xy plane. The dashed line indicates the longitudinal channel symmetry axis.

the coolant flow velocity and, hence, on the cooling efficiency, can be neglected.

The calculations showed that the coolant velocity insignificantly changes along the channel length, which is very important for uniform cooling of the active elements of LDAs. As is known, the laminar flow velocity is inversely proportional to the cross section area. In our case of the turbulent flow in the channels between LDBs, this velocity is 2.2 times higher than the initial velocity at the entrance to the inlet funnel (10 and 15 m s^{-1}) and is 22 and 33 m s^{-1} , respectively, in the centre of the channel cross section. Thus, the fluid flow is turbulent, which makes the heat transfer more efficient. The coolant flow velocity distribution (Fig. 2b) noticeably differs from parabolic, i.e., the velocity near the channel wall increases considerably faster, which is typical for turbulent flows.

Due to the turbulent character of the flow, its velocity at a distance of less than 1 μm from the wall (metallised surface of the LDB crystal) at the initial flow velocity of 15 m s^{-1} is 2.7 m s^{-1} and rapidly increases reaching 15 m s^{-1} at a distance of only 2.5 μm , which ensures a high heat transfer efficiency. At the initial flow velocity of 10 m s^{-1} , the velocity near the wall is 1.9 m s^{-1} , and the 15- m s^{-1} velocity is achieved by the flow at a distance of 5.5 μm from the wall.

Of special interest for solving the posed problem is the distribution of temperature fields in the LDA, in particular, in

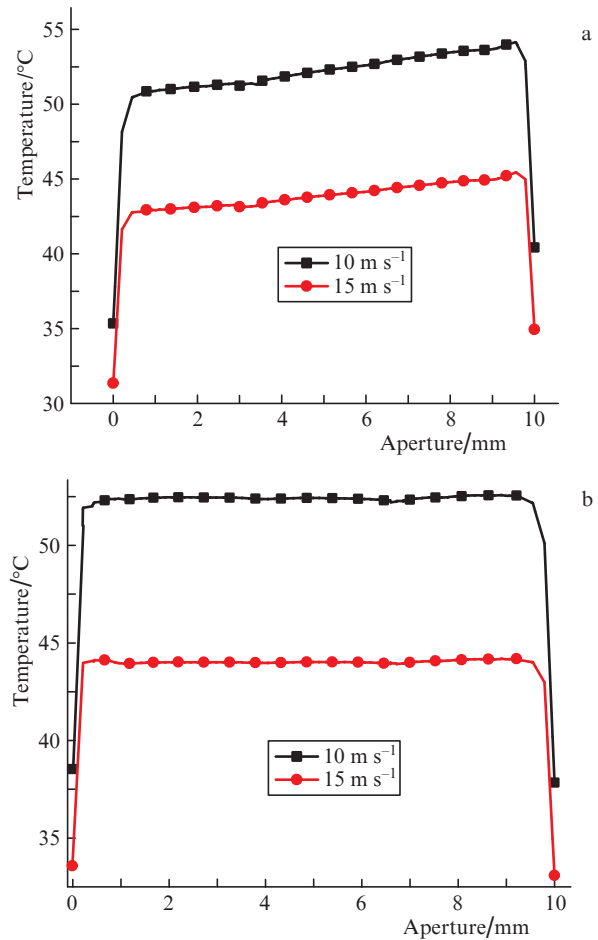


Figure 3. Average temperature of the active region over the LDA aperture for (a) UD and (b) CD flows.

the LDBs. Figure 3 shows the temperature distribution in the LDB active region calculated for two initial velocities of the UD and CD coolant flows.

Zero on the horizontal axis in Fig. 3 (y axis directed along the channel) corresponds to the entrance to the channel. One can see that, in the case of UD coolant flows, the thermal field is nonuniform and its amplitude in the LDB active region increases in the direction of the channel exit. Since the cooling fluid temperature increases as it propagates in the channel along the hot active region of the LDB, the cooling efficiency decreases in the direction of the channel exit. Moreover, as the flow velocity increases from 10 to 15 m s^{-1} , the maximum temperature of the LDB active region decreases from 54 to 45 $^{\circ}\text{C}$, and the average temperature gradient decreases from 3.5 to 2 $^{\circ}\text{C}$ (Fig. 3a).

Calculations of the average and maximum temperatures in the LDB active region at coolant flow velocities of 10 and 15 m s^{-1} at the entrance to the channel showed that the average temperature is almost identical for both UD and CD flows, while the maximum temperature in the case of UD flows exceeds the corresponding temperature in the case of CD flows by no more than 1.5 $^{\circ}\text{C}$. The maximum temperatures for both type of flows with the considered initial velocities lie in the temperature range 45–55 $^{\circ}\text{C}$, which is acceptable for reliable LDB operation, and these temperatures for CD flows are lower than for UD ones by, on average, 1 $^{\circ}\text{C}$. Thus, the main advantage of cooling by CD flows, i.e., a better uniformity of the thermal field distribution over the aperture,

leads to a decrease in the thermoelastic stress and to better uniformity of the LDB output parameters. The latter circumstance is especially important for spectral summation used to increase the LDA brightness.

4. Comparison of the direct convective method of LDB cooling with conductive cooling methods

Two-side cooling of LDBs has been known since long ago and provides higher efficiency and a more uniform temperature distribution but is more difficult to implement technically. As was mentioned above, as a structural element of an LDA, it was proposed in [5, 6] to use a sandwich consisting of an LDB crystal between two thermal compensators. It is a scheme of two-side conductive heat transfer. As far as we know, our scheme of direct convective cooling of LDBs by a coolant, including the scheme using alternating CD flows in one plane, is considered for the first time.

Figure 4 shows the temperature profiles in the cross section of the active LDB region with dimensions 2×10 mm at a thermal load of 100 W in the case of mounting both directly on a copper heat sink (Cu) and with intermediate thermal compensators and submounts based on CuW, AlN, and synthetic diamond with a thermal conductivity of $100 \text{ W m}^{-1} \text{ K}^{-1}$,

as well as in the case of direct two-side cooling of LDBs (in the composition of an LDA consisting of 50 LDBs) by CD water flows with a velocity of 15 m s^{-1} .

One can see from Fig. 4 that, at standard mountings, the UD heat fluxes from the active region and the position of the output mirror at the heat sink edge lead to a pronounced non-uniformity of the thermal field; in this case, the temperature gradient may reach 20°C over the LDB aperture and 14°C along the cavity length. Naturally, the higher the thermal conductivity of the submount or thermal compensator, the lower the maximum temperature and nonuniformity of the thermal field. In particular, at identical thermal loads, the maximum temperature in the region of the central LDB clusters exceeds 60°C in case of using a CuW temperature compensator and 50°C in the case of a diamond submount. Nevertheless, even in the latter case, the temperature gradient along the cavity length (2 mm) is about 7°C .

The dependences shown in Fig. 4 convincingly demonstrate the qualitative and quantitative advantages of the proposed ‘coolant mounting’. Our mounting variant, in addition to the possibility of reducing the thermal load on the LDB mirrors due to the two-side heat removal from the LDA and additional cooling by structural elements (which is impossible in standard designs), provides excellent thermal field uniformity over the aperture and along the cavity length. In this case, the average LDB temperature is 10°C lower than when using a synthetic diamond submount. These advantages are important for increasing the LDA reliability because the larger the temperature gradient, the higher thermoelastic stresses in both the LDB itself and the soldering interfaces between the structural elements due to their different thermal expansion coefficients. ‘Coolant mounting’ minimises these problems. As a result, we have an almost plane temperature profile in the active region cross section over the aperture and the temperature of LDB mirrors 7°C lower than the temperature in the middle of the cavity.

5. Conclusions

The calculations and analysis of the obtained results show considerable advantages of the new method of direct cooling of LDBs by a coolant. It should be noted that in our model we used LDBs with intentionally reduced parameters (cw power 100 W, total efficiency 50%), but, nevertheless, the calculated optical cw power density of the LDA was 5 kW cm^{-2} at a coolant temperature of 20°C , which exceeds published records by 2.5 times. We estimate that, using LDBs described in the aforementioned works (power 250 W, total efficiency 65%–70%) and increasing the packing density of LDBs in the array, we may achieve the calculated power density of LDAs of our design exceeding 15 kW cm^{-2} .

It is obvious that, at present, the practical implementation of the proposed design is a complicated engineering problem related to the development of new and, probably, expensive technologies of LDA assembling. This includes, in particular, mounting of LDBs, providing hermetic sealing, formation of turbulent CD coolant flows in neighbouring channels, minimisation of thermoelastic stresses, increasing the LDB packing density in the LDA to increase the output power density, etc. This raises the question of to what extent the advantages of the LDAs of the new design will be able to compensate for the problems with their fabrication. The present work partially answers this question.

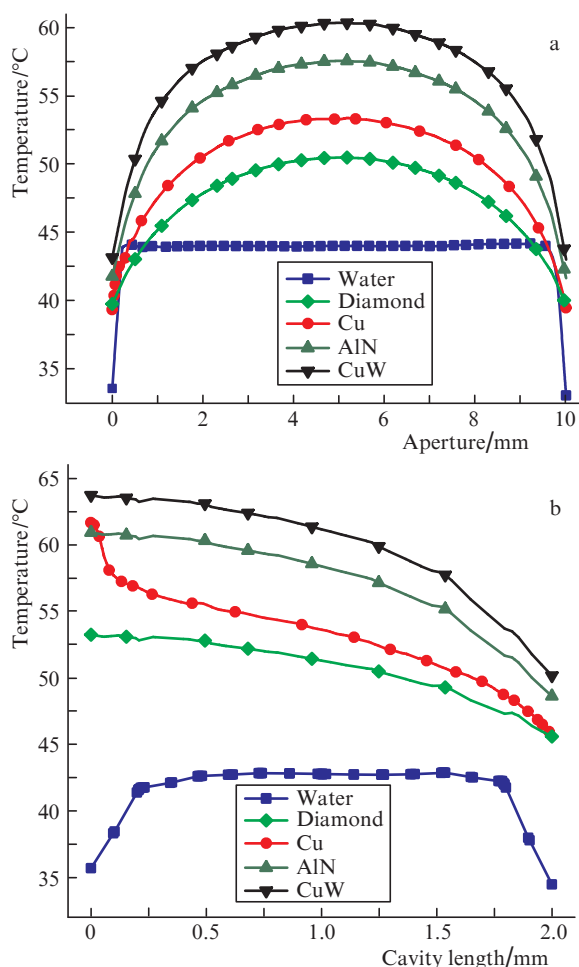


Figure 4. Temperature profiles in the LDB active region cross section along (a) the emitting aperture and (b) the cavity length. The output cavity mirror in Fig. 4b is on the left.

Acknowledgements. The authors thank G.T. Mikaelyan and E.A. Cheshev for collaboration and O.V. Revinskii for patent preparation.

References

1. Veselov D.A., Pikhtin N.A., Lyutetskii A.V., Nikolaev D.N., Slipchenko S.O., Sokolova Z.N., Shamakhov V.V., Shashkin I.S., Kapitonov V.A., Tarasov I.S. *Quantum Electron.*, **45**, 7 (2015) [*Kvantovaya Elektron.*, **45**, 7 (2015)].
2. Ladugin M.A., Marmalyuk A.A., Padalitsa A.A., Bagaev T.A., Andreev A.Yu., Telegin K.Yu., Lobintsov A.V., Davydova E.I., Sapozhnikov S.M., Danilov A.I., Podkopaev A.V., Ivanova E.B., Simakov V.A. *Quantum Electron.*, **47**, 4 (2017) [*Kvantovaya Elektron.*, **47**, 4 (2017)].
3. Strohmaier S.G., Erbert G., Meissner-Schenk A.H., Lommel M., Schmidt B., Kaul T., Karow M., Crump P. *Proc. SPIE*, **10086**, 100860C (2017).
4. Frevert C., Bugge F., Knigge S., Ginolas A., Erbert G., Crump P. *Proc. SPIE*, **9733**, 97330L (2016).
5. Fassbender W., Lotz J., Kissel H., Biesenbach J. *Components Packaging for Laser Systems IV*, **10513**, 105130M (2018).
6. Zhang Hongyou, Cai Lei, Zah Chung-en, Liu Xingsheng. *Proc. SPIE*, **11182**, 111820F (2019).
7. Bezotosnyi V.V., Kozyrev A.A., Kondakova N.S., Kondakov S.A., Krokhin O.N., Mikaelyan G.T., Popov Yu.M., Cheshev E.A. *Bull. Lebedev Phys. Inst.*, **43**, 369 (2016) [*Kratk. Soobshch. Fiz. FIAN*, **43** (12), 41 (2016)].
8. Gongnan Xie, Yanquan Liu, Sunden Bengt, Zhang Weihong. *J. Therm. Sci. Eng. Appl.*, **5**, 011004 (2013).
9. Holmes M.J., Parker N.G., Povey M.W. *J. Phys.: Conf. Ser.*, **269**, 012011 (2011).
10. CFD Module User's Guide. Comsol (2018); <https://doc.comsol.com/5.4/doc/com.comsol.help.cfd/CFDModuleUsersGuide.pdf>.